Characterization of angiogenesis and inflammation surrounding ePTFE implanted on the epicardium

Robert S. Kellar, Leigh B. Kleinert, Stuart K. Williams
Biomedical Engineering Program, University of Arizona, 1501 North Campbell Avenue, Tucson, Arizona 85724-5084

Received 14 February 2001; revised 17 July 2001; accepted 26 July 2001

Abstract: The response of epicardial tissue to the implantation of expanded polytetrafluoroethylene (ePTFE) was evaluated and compared with identical material implanted within subcutaneous and adipose tissues. These two tissue environments were selected for comparison with epicardial implants because they represent tissue often involved in device implantation. Discs of ePTFE (6 mm) were implanted into three different tissue sites in Sprague-Dawley rats. At 5 weeks, polymers and surrounding tissues were harvested and processed for light microscopy. General histology and histochemistry data indicated all polymers to be well incorporated with new tissue. Subcutaneous implants were covered by a dense fibrous capsule (55–70 μm). Epicardial and adipose implants had no fibrous capsule and a significantly greater number of microvessels (arterioles, capillaries, and venules) within the surrounding tissues compared with subcutaneous implants. An increased level of inflammation was also observed around epicardial implants compared with the other implants. Additionally, the new vasculature surrounding epicardially implanted ePTFE revealed an altered microvessel density and vessel type distribution compared with normal (control) epicardium. These results suggest that epicardial tissue responds to implanted ePTFE with a robust inflammatory response that may support the formation of a new microvasculature that is uniquely different from the native epicardial microvasculature. © 2002 Wiley Periodicals, Inc. J Biomed Mater Res 61: 226–233, 2002

Key words: angiogenesis; epicardium; ePTFE; vessel density; vessel characterization

INTRODUCTION

Historically, biomedical implants have been developed with a primary design emphasis on structural characteristics and a secondary emphasis for material biocompatibility. With the increased understanding of tissue responses to implanted materials, it has become evident that the current and future evaluation of biomedical implants needs to include the healing response elicited by these materials after their implantation into biological tissues. Preclinical analyses of polymer-induced healing commonly use an animal model where the implant is placed in a subcutaneous pocket.[1,2] The healing response elicited within subcutaneous tissue is often considered indicative of the healing that would be observed in any anatomic site. Other studies, however, have demonstrated tissue-site specific healing responses in response to material implants.[3] The future analysis of the healing response evoked by polymeric implants should specifically consider the tissue into which the device is planned for final clinical use.

When considering the use of polymers, specifically expanded polytetrafluoroethylene (ePTFE) implanted onto the epicardial surface, it is important to first evaluate the evoked healing response by the epicardium. This healing response may affect the success of the implant because of the recruitment of inflammatory cell types or microvascular elements. Expanded PTFE devices that come in contact with the epicardial tissue environment include pericardial patches, pericardial wraps, and coronary artery bypass grafts (CABG). Pericardial patches can be used as a surgical membrane to assist with closure of the pericardium after open chest surgery or to help minimize tissue adhesion surrounding the heart for future repeat operations.[4,5] Future applications for these devices may include revascularization of, or delivery of drugs to, damaged or weakened myocardium. Pericardial wraps are used in cases of heart failure as a physical support around the heart.[6] Finally, the development of a synthetic CABG continues to be a goal of many investigators in the hopes of developing an autologous vessel substitute.[7,8] These examples of ePTFE devices within the epicardial tissue environment raise impor-

Correspondence to: S. K. Williams; e-mail: skwill@u.arizona.edu

tant questions regarding how the epicardium responds to ePTFE implantation.

Therefore, evaluation of two features of the healing response, specifically inflammation and angiogenesis, after ePTFE implantation onto the epicardium will provide biocompatibility data that may help to improve currently used and future ePTFE devices. Inflammation (defined as the presence of activated macrophages and foreign body giant cells) and the formation of a fibrous capsule are tissue-specific parameters that have been a focus of investigators' efforts in the evaluation of biomedical implants.[9,10] Additionally, the evaluation of angiogenesis (the development of new blood vessels from pre-existing vessels) in the peri-implant area has been realized as an important parameter for influencing the polymer-tissue interface.[11,12] Promoting new blood vessel development within and surrounding currently used polymeric devices may contribute to their long-term function by providing appropriate nutrient and waste product exchange to the surrounding tissues. In the case of a vascular graft, transinterstitial growth of blood vessels may also allow for the establishment of a quiescent endothelial lining on the lumenal (blood contacting) surface.[11,13]

Previous methods for the quantitation of the angiogenic response associated with polymer implants often use an index or numerical value based on a microvessel density, expressed as the number of vessels per high powered field (a defined area).[14,15] This analysis yields important quantitative information regarding vessel density. However, the development of a functional new microvasculature in response to polymer implantation may require more than just the establishment of a tissue with an increased vascular density. For example, the metabolic needs of a healing tissue may require a specific vascular complexity that includes microvascular density as well as microvessel types. The distribution of these vessel types alludes to the physiological demands and thus the functionality of the new vasculature in the healing tissue. Consequently, we have expanded our evaluation of the vascular response associated with implanted materials to examine these parameters. This analysis specifically characterizes the type of vascular/angiogenic response associated with a biomedical implant, thereby providing information on the physiological role of the new vasculature.

In the current study, we have evaluated the healing response associated with ePTFE implanted onto the epicardial surface, and compared these data to tissue responses elicited by ePTFE implanted in other tissues. The goal of this study was to evaluate the inflammation and vascular response in tissue that forms around these materials, including the parameters of microvessel density and type. The data support the conclusion that the healing response, with respect to microvessel density, inflammation, and vessel type distribution, in association with ePTFE implants, is dependent on the tissue environment.

MATERIALS AND METHODS

Study design

All animal studies were performed after approval of protocols by the Institutional Animal Care and Use Committee. National Institutes of Health (NIH) Guidelines for the Care and Use of Laboratory Animals (NIH publication 85-23, revised 1985) were observed. Animals were housed in American Association for the Accreditation of Laboratory Animal Care approved facilities. Male Sprague-Dawley rats weighing 300 to 400 g were used for the implant experiments. Five rats received ePTFE implants on the epicardial surface. Seven separate rats received ePTFE implants in adipose tissue and subcutaneous tissue sites. Samples from all three tissue sites were explanted after 5 weeks. Samples were subsequently evaluated morphologically and immunocytochemically.

Implant surgery

General anesthesia was induced and maintained by an intraperitoneal injection of pentobarbital. Implant sites were prepared by removing hair and the area was cleaned using Nolvasan. Sterility was maintained and a warming pad was used throughout the procedure. Sterile, 6-mm discs that were punched out of ePTFE vascular grafts (Impra Corp., Tempe, AZ; standard wall thickness, 30-micron internodal distance) were implanted into the three different tissue sites.

For epicardial implants, the rats were intubated using a laryngoscope to allow for ventilated respiration. Epicardial implantation was accomplished by performing a sternotomy. As soon as the pleural membrane was pierced, the rat was immediately connected to the ventilator for artificial respiration of the lungs. The ventilator (Harvard Rodent Ventilator Model 683) was set to deliver 2.6 mL of air at 90 breaths per minute. On the heart's surface, the pericardial sac was gently pulled away from the epicardium and a small hole (3 mm) was made through the pericardial sac. The ePTFE disc was sutured onto the epicardium with the ablumenal (non-blood contacting) side of the disc in contact with the heart surface. The chest was closed in three layers with a chest evacuation tube in place. The chest was evacuated, ventilator stopped, and animal recovered.

Implants in the subcutaneous and adipose sites followed the previously published procedures of Williams et al.[16] Briefly, subcutaneous implantation was accomplished by making a 1.0-cm incision in each dorsal lumbar region and a subcutaneous pocket was formed. Discs were implanted and the incision was closed with metal auto-clips. Fat implants were performed by making a midline incision in the abdomen, followed by exposure of the distal two-third portion of

each epididymal fat pad. One disc of ePTFE per fat pad was placed onto the fat and the tissue was then approximated using 5-0 Prolene® (Ethicon Corp.) suture. The midline incision was closed in two layers and animal recovered.

Explant and evaluation

Five weeks after polymer implantation, general anesthesia was administered using pentobarbital. The polymers and a significant portion of the surrounding tissue were exposed and removed. Samples were immediately immersed into Histo-Choice® (Ameresco, Solon, OH) fixative. Samples were dehydrated, brought to paraffin, and block embedded. Sections (6 μm) were subsequently processed for light microscopic evaluation by staining with hematoxylin and eosin (H&E), and photomicrographs were obtained.

Sections for histochemical evaluation were reacted with ED1 antibody, specific for activated monocytes, macrophages, and foreign body giant cells (monoclonal, mouse anti-rat ED1; Harlan, Inc.) used at a final dilution of 1:200. Primary antibody was visualized using a secondary antibody with a peroxidase reaction product recognition system (Universal mouse kit; Dako, Inc.). Separate sections were evaluated using the lectin *Griffonia simplicifolia* to identify vascular elements (peroxidase conjugated lectin-Gs-1; EY Laboratories used at a final concentration of 1:100). The Gs-1 lectin binding was visualized using a peroxidase reaction product. Finally, separate sections were reacted with an alpha smooth muscle cell actin antibody (Sigma, Inc.; used at a final concentration of 1:400) to identify smooth muscle within the microvascular wall. For these sections, primary antibody was visualized using the secondary antibody with a peroxidase reaction product recognition system. For all three histochemical techniques (ED1, Gs-1, and smooth muscle cell actin), a methyl green counter stain was used to identify background nuclei.

Microvessel density/inflammatory cell density

The tissue-implant interface, corresponding to the ablumenal ePTFE-epicardial surface, was viewed using a 40× water immersion lens for vasculature and inflammatory cells. For microvessel density counts, the number of cross sectional and longitudinal blood vessel profiles per high magnification (HM = 54 × 54 μm) was counted. Each HM area analyzed included an area 54 × 54 μm from the ePTFE material into the tissue (the interstices were not evaluated). Ten random HM counts were taken along the entire length of the tissue-graft interface of the ePTFE (n = 5 per group). The criteria for the positive count of a vessel were: 1. positive Gs-1 reaction, 2. an identifiable lumen, and 3. within the designated high magnification. An eyepiece grid measuring 54 × 54 μm (2.9×10^{-3} mm^2) was used to visually define the HM borders. The number of vessels per mm^2 was calculated and reported.

For inflammatory cell density counts, the number of ED1 positive reacting cells was quantified using the same procedure. A one-way ANOVA and a Bonferroni *post hoc* statistical test were used to determine significance between treatment groups.

Microvessel type analysis

Sections treated with Gs-1 were analyzed under a light microscope with a 20× lens. The ablumenal side of the tissue–implant interface of the ePTFE was analyzed for microvessel typing. Five random HM (200 × 200 μm) counts were identified along the length of the tissue–graft interface of the ePTFE (n = 5 per group). Microvessels were classified using standard histologic features.[17] Arterioles were identified by the presence of the characteristic layers: the endothelium, internal elastic membrane, tunica media consisting of one or more smooth muscle layers, tunica adventitia, and an internal diameter ≥10 μm. Capillaries were identified by their single layer of flattened endothelial cells.[17] Venules were differentiated from arterioles by their large lumen diameter in comparison to vessel wall thickness, a thinner or absent smooth muscle layer, a less significant tunica adventitia, and an internal diameter >10 μm. Internal diameter measurements were taken using NIH SCION Image software.

RESULTS

Histology

After explant (5 weeks), examination of general histology revealed all polymers to be well incorporated with new tissue in all implantation sites. Subcutaneous implants exhibited a covering of a dense avascular fibrous matrix (capsule) with a relative thickness of approximately 55–70 μm that was found to be composed predominantly of extracellular matrix [Fig. 1(C)]. Minimal cell presence in the interstices of the ePTFE was observed by H&E staining. In contrast, the tissue surrounding adipose implants showed no evidence of a fibrous capsule after the 5 weeks of implantation. Furthermore, epicardial implants were associated with a vascularized granulation tissue containing cellular and acellular components. [Fig. 1(A,B)]. Adipocytes were observed in close proximity to the adipose implants and connective tissue with nucleated cells were seen in close association to epicardial implants. A significant number of cells were observed within the interstices of the ePTFE in both adipose and epicardial tissues and identifiable microvessel profiles were in close association to the polymers in these two tissues. However, by H&E analysis, a limited number of microvessels were found within the interstices of the polymers in all three tissue sites of implantation.

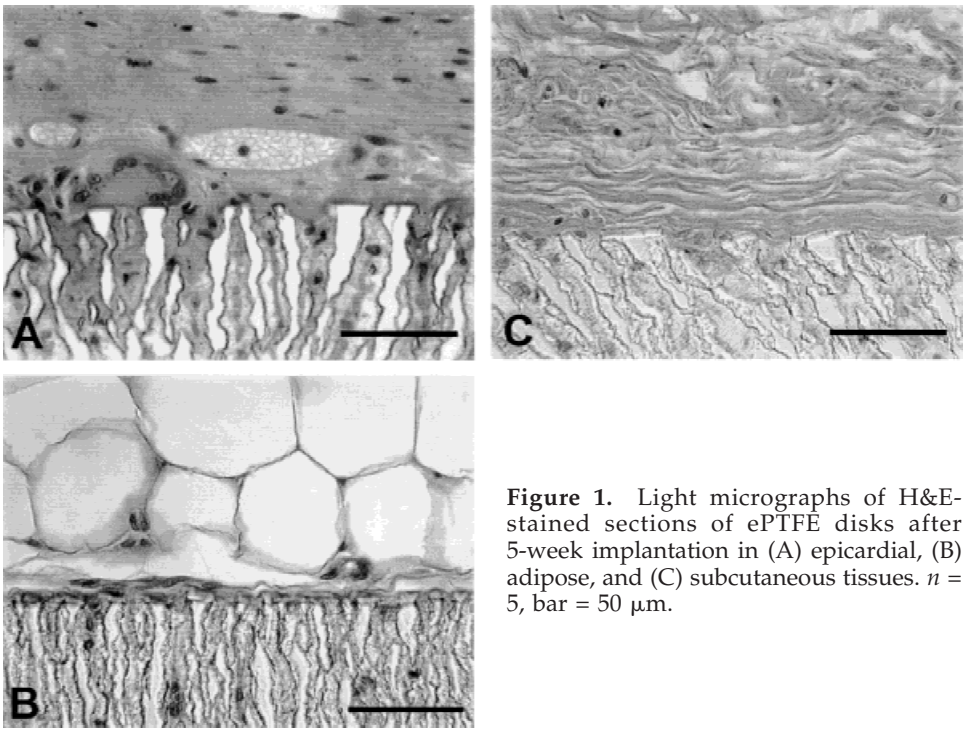

Figure 1. Light micrographs of H&E-stained sections of ePTFE disks after 5-week implantation in (A) epicardial, (B) adipose, and (C) subcutaneous tissues. n = 5, bar = 50 μm.

Histochemistry

Analysis of separate sections of tissues reacted with Gs-1 lectin revealed a greater number of new microvessels within the surrounding tissue of epicardial and adipose implants compared with subcutaneous implants [Fig. 2(A,C)]. This observation was validated by a higher number of Gs-1 positive microvessels within the surrounding tissues of epicardial and adipose implants. These blood vessels were observed in both cross sectional or longitudinal orientations. In addition, sections stained with ED1 antibody revealed a greater number of ED1 positive inflammatory cells in close association to epicardial implants compared with adipose and subcutaneous implants [Fig. 3(A,C)].

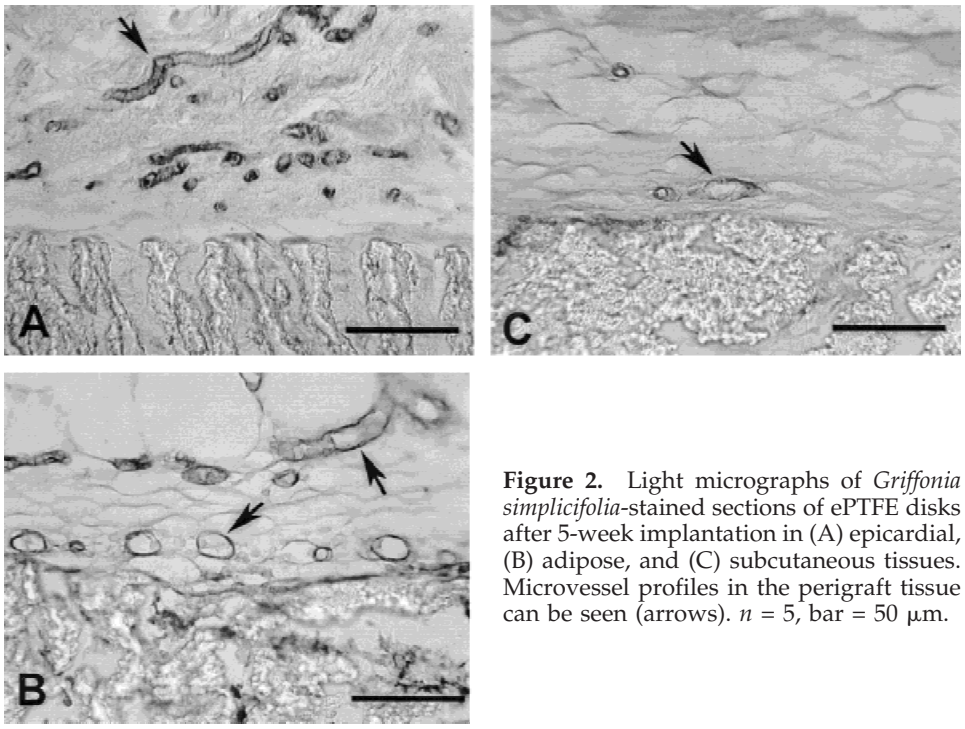

Figure 2. Light micrographs of *Griffonia simplicifolia*-stained sections of ePTFE disks after 5-week implantation in (A) epicardial, (B) adipose, and (C) subcutaneous tissues. Microvessel profiles in the perigraft tissue can be seen (arrows). n = 5, bar = 50 μm.

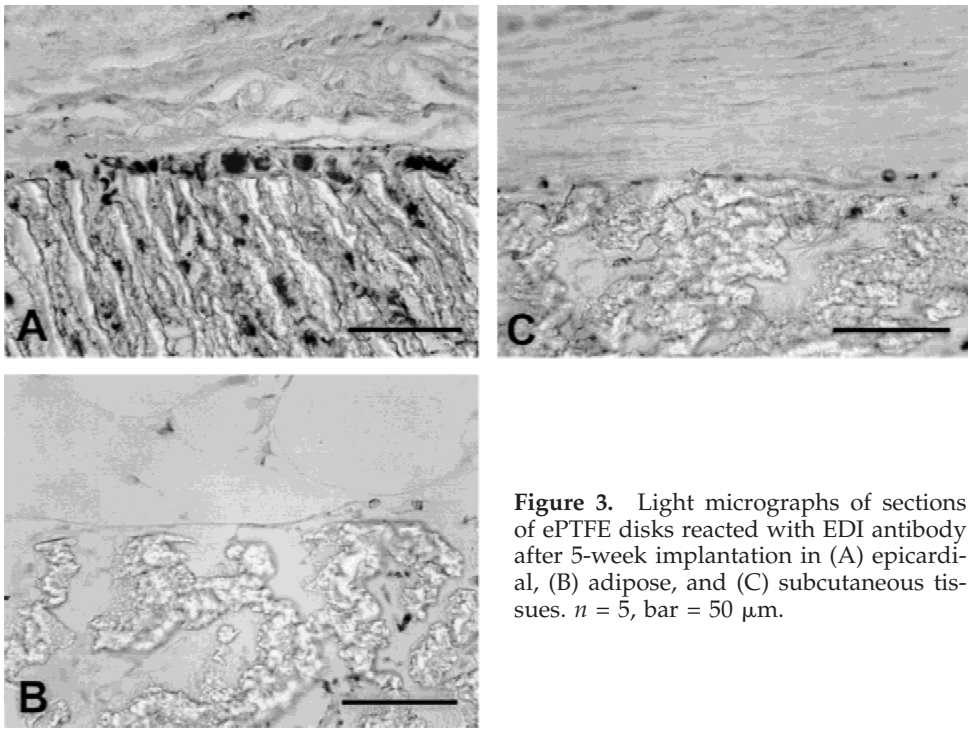

Figure 3. Light micrographs of sections of ePTFE disks reacted with EDI antibody after 5-week implantation in (A) epicardial, (B) adipose, and (C) subcutaneous tissues. $n = 5$, bar = 50 μm.

Morphometric evaluation of the vascular response and inflammation

Slides reacted with the Gs-1 lectin and ED1 antibody were subjected to morphometric analysis of microvessel density (microvessels/HM) and inflammatory cell density (inflammatory cells/HM). Figure 4 illustrates the microvessel density in tissue formed around ePTFE implants within the three different tissue sites tested. These data demonstrate a significantly higher microvessel density in the tissues around epicardial and adipose ePTFE implants compared with the subcutaneous tissue site. Evaluation of microvessel densities from normal (control) epicardium, adipose, and subcutaneous tissues were also performed. Comparisons of these control microvessel densities showed no significant difference. However, direct comparisons of control tissue microvessel densities to the corresponding implant associated tissue reveal significant differences between the epicardial and adipose tissue groups (Fig. 4). Figure 5 illustrates the inflammation in tissue formed around ePTFE implants within the three different tissues. The ED1 antibody was used to identify activated macrophages and foreign body giant cells. Analysis of these data indicate a significantly higher level of inflammation (primarily

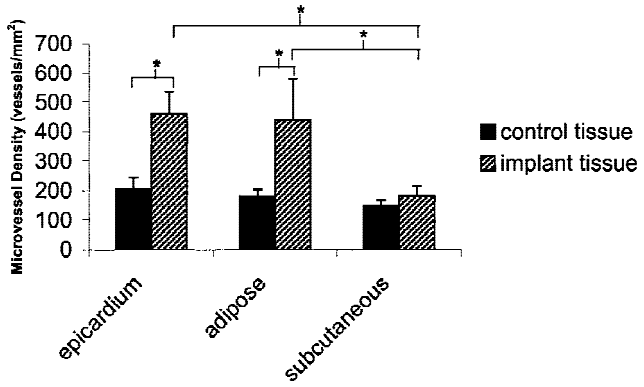

Figure 4. Microvessel densities of control (nonimplanted) epicardial, adipose, and subcutaneous tissues (shown in solid bars). Microvessel densities of the peri-implant tissue surrounding ePTFE disks after 5-week implantation in epicardial, adipose, and subcutaneous tissue (shown in hatched bars). $n = 5$, $p \leq 0.05$.

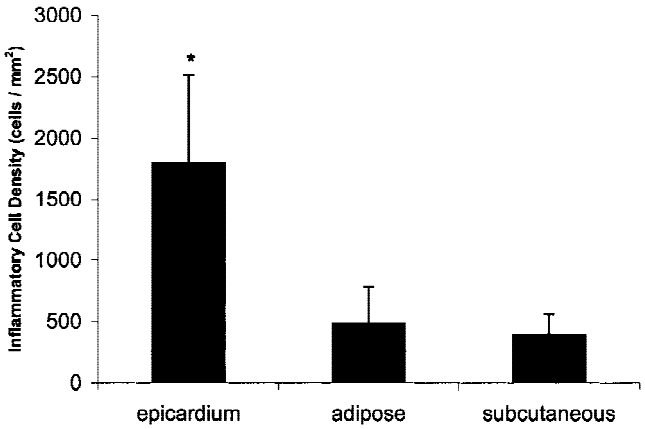

Figure 5. Inflammatory cell densities of the peri-implant tissue surrounding ePTFE disks after 5-week implantation in epicardial, adipose, and subcutaneous tissues. $n = 5$, $p \leq 0.05$.

activated macrophages) around epicardial implants compared with adipose and subcutaneous implants. Additionally, a greater number of foreign body giant cells were observed around epicardial implants when compared with adipose and subcutaneous implants (Fig. 1). Values for control tissues are not shown because in normal tissues the inflammatory cell numbers are negligible.

Microvessel types

The microcirculation of normal tissue exists as a balance of microvascular types, arterioles, capillaries, and venules. In this study, the microvessel types within the healing tissues around the ePTFE implants were characterized and compared with the microvessel distributions within normal (control) tissues. Table I demonstrates that the microvascular environment of control epicardium exhibits a distribution in the rank order of venules, capillaries, and arterioles. In contrast, the microvessels that predominate in tissue formed around epicardial ePTFE implants are capillaries, followed by venules, and arterioles. The major differences in vessel type distribution of the epicardium are found with a shift from 57.38 ± 3.16% venules in control epicardium to 25.34 ± 7.33% venules in epicardial tissues around ePTFE implants. Additionally, the capillary presence increased from 32.79 ± 1.22% in control epicardium to 60.62 ± 12.30% in implanted epicardial tissues. Furthermore, the microvascular environment of control adipose tissue and the adipose tissues around ePTFE implants were found to be primarily capillaries, secondarily venules, and arterioles. Finally, within control subcutaneous tissues and subcutaneous tissues around ePTFE implants, these environments were found to support a majority of capillaries, then arterioles, and finally venules. Figure 6 illustrates the types of microvessels present in tissues around epicardial, adipose, and subcutaneous tissues.

TABLE I
Relative Percent of Microvessel Types

	Control Epicardium	Implant Epicardium
% arterioles	9.84 ± 0.84	13.70 ± 1.41
% capillaries	32.79 ± 1.22	60.62 ± 12.30
% venules	57.38 ± 3.16	25.34 ± 7.33
	Control Adipose	Implant Adipose
% arterioles	3.33 ± 0.58	15.44 ± 2.49
% capillaries	90.00 ± 1.91	63.97 ± 5.37
% venules	6.67 ± 0.96	20.59 ± 2.19
	Control Subcutaneous	Implant Subcutaneous
% arterioles	17.93 ± 3.70	25.00 ± 3.40
% capillaries	66.67 ± 4.92	63.46 ± 3.30
% venules	15.40 ± 1.63	11.54 ± 3.00

DISCUSSION

In this study, an epicardial model for the evaluation of polymer healing was developed and used to evaluate the healing response associated with clinically available ePTFE material. The healing responses observed suggest that the epicardial tissue environment is capable of initiating and supporting a significant angiogenic and inflammatory reaction in response to ePTFE implantation. These data were compared with current existing models of polymer evaluation, specifically the subcutaneous and adipose tissue models of polymer evaluation.

The epicardial tissue environment represents a surface that comes in contact with a variety of biomedical devices. Some of these devices that have been previously mentioned include pericardial patches, pericardial wraps, and synthetic CABGs. The development of synthetic CABGs has received great attention because of the vast patient population that may benefit from an autologous vessel substitute. Significant effort has focused on the lumenal aspects of CABG with little emphasis placed on the ablumenal tissue interactions.[18–20] Expanded PTFE as a long-term substitute for CABG has seen limited success in the patient population.[7,8] Although lumenal patency remains an important objective for CABG, we propose that the ablumenal tissue responses may influence lumenal characteristics. Our current study evaluated the ablumenal cellular interactions that occur around peripheral and coronary placed ePTFE polymers. These data contribute information about the cellular composition around these implanted polymers and how the healing responses may affect ablumenal tissue remodeling and lumenal characteristics.

The ablumenal healing responses, specifically inflammation and angiogenesis, may directly affect lumenal patency by cellular activation through cytokine or growth factor production. Therefore, a contributing factor to ePTFE's failure as a small caliber coronary graft may be the recruitment of activated macrophages around epicardially implanted ePTFE and the ability of these inflammatory cells to migrate into the interstices of the graft material where they can elicit a lumenal response. These inflammatory macrophages are known to release a number of cytokines, including platelet activating factor, interleukin-1, and platelet-derived growth factor, which are known to activate platelets, the coagulation cascade, and smooth muscle cell proliferation (leading to intimal thickening), respectively.[21,22] These same macrophages are capable of releasing numerous known angiogenic growth fac-

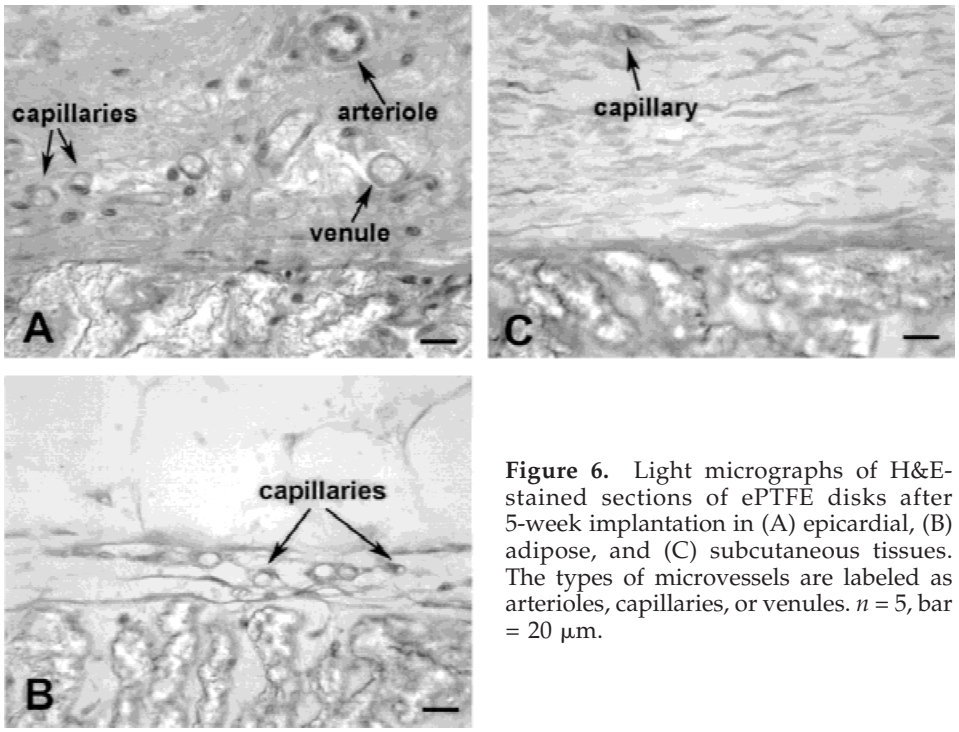

Figure 6. Light micrographs of H&E-stained sections of ePTFE disks after 5-week implantation in (A) epicardial, (B) adipose, and (C) subcutaneous tissues. The types of microvessels are labeled as arterioles, capillaries, or venules. $n = 5$, bar = 20 μm.

tors,[21,22] which may be responsible for the dramatic angiogenic response around epicardially implanted ePTFE. The concomitant release of thrombotic factors and angiogenic factors may be contributing to lumenal thrombosis and intimal thickening while stimulating a new microvasculature around these implants to recruit additional inflammatory macrophages. These interpretations of the data support previous authors who suggest a codependence of inflammation and angiogenesis.[22–24]

During the evaluation of the angiogenic response, the microvessel density and type was characterized. With reference to microvessel density, the benefits of stimulating a microvascular bed around polymer implants include the local delivery of nutrients and removal of waste products. Additionally, in the case of a vascular graft, the ability to promote neovascularization of the polymeric material may allow for the transmural migration of endothelial cells to establish a quiescent, anti-thrombotic lumenal monolayer. When evaluating the importance of microvessel type characterization, it is necessary to consider the microvasculature throughout the body where different physiological demands require a specialized vasculature. For example, metabolically active tissues, such as cardiac muscle, require a high density of capillary exchange vessels for the efficient delivery of oxygen and removal of carbon dioxide and other metabolic waste products. Collectively, the parameters of microvessel density and type help shape the physiological function of the vasculature by providing few or numerous vessels within the tissue in a variety of vessel type distributions according to the needs of the perfused tissue. Therefore, characterization of the vascular response in this study included an evaluation of these parameters within normal (control) tissues and implanted tissues.

Microvessel type evaluation suggests a physiological function of the new microvasculature within control tissues and tissues surrounding ePTFE implants. For example, the epicardial surface represents a tissue bed that is primarily dominated by mid-sized drainage venules. Physiologically, these venules could serve as fluid collection reservoirs to assist in the return of interstitial fluid into the circulation. Whereas a mature microvasculature is seen around epicardial ePTFE implants with the presence of arterioles, capillaries, and venules, after 5 weeks of ePTFE polymer implantation, the new tissue environment is dominated by capillaries that physiologically serve as gas and nutrient exchange vessels. The differences in the microvessel type distributions between control epicardium and the tissue surrounding epicardial implants suggest either that the physiological needs of the healing tissues favor gas and nutrient demands over interstitial fluid balance or insufficient signals are present for the complete maturation of all new microvessels. For the design of biomedical implants that stimulate the formation of a new vasculature, it may be important to model the surrounding vascular bed of normal tissue (with respect to vessel density and type). In this way, the formation of a vascular response that mimics the normal tissue will allow for the proper function of the vasculature and thus help to

improve the biocompatibility of the material. In cases in which ePTFE is being used on the epicardial surface as a cardiac repair patch, pericardial wrap, drug delivery device, or as a synthetic CABG, modifications of this material may be necessary to promote either a noninflammatory condition or an angiogenic response that mimics the normal tissue.

In this study, the healing response surrounding epicardially implanted ePTFE materials was characterized and compared with previously reported tissue sites of polymer implantation, adipose, and subcutaneous tissues. This study contains novel data that allow for characterization of the healing response associated with ePTFE materials in the epicardial position. Additionally, this study has focused on the angiogenic response surrounding implanted ePTFE material by quantifying microvessel density as well as characterizing the types of blood vessels present in the regenerating tissues surrounding these implants. These data indicate that the epicardial tissue environment responds to ePTFE implantation with a unique healing response. Therefore, the evaluation of ePTFE devices that will reside on the epicardium needs to consider the inflammatory and angiogenic responses evoked by epicardial tissues.

References

1. Okamoto T, de Castro AL, dos Santos PR, Moroni P. Silicone implantation into subcutaneous connective tissue: Histological study in rats. Rev Fac Odontol Aracatuba 1975;4:91–97.
2. Walboomers XF, Jansen JA. Microgrooved silicone subcutaneous implants in guinea pigs. Biomaterials 2000;21:629–636.
3. Williams SK, Berman SS, Kleinert LB. Differential healing and neovascularization of ePTFE implants in subcutaneous versus adipose tissue. J Biomed Mater Res 1997;35:473–481.
4. Bhatnagar G, Fremes SE, Christakis GT, Goldman BS. Early results using an ePTFE membrane for pericardial closure following coronary bypass grafting. J Cardiovasc Surg 1998;13: 190–193.
5. Lahtinen J, Satta J, Pokela R, Nissinen J, Juvonen T. Pericardial closure with polytetrafluoroethylene surgical membrane or biodegradable polyglycolic acid mesh after coronary artery bypass surgery: A baseline report. Ann Chir Gynaecol 1998;87: 36–39.
6. Power JM, Raman J, Dornom A, Farish SJ, Burrell LM, Tonkin AM, Buxton B, Alferness CA. Passive ventricular constraint amends the course of heart failure: A study in an ovine model of dilated cardiomyopathy. Cardiovasc Res 1999;44:549–555.
7. Chard RB, Johnson DC, Nunn GR, Carmill TB. Aorta-coronary bypass grafting with polytetrafluoroethylene conduits. J Thorac Cardiovasc Surg 1987;94:132–134.
8. Sapsford RN, Oakley GD, Talbot S. Early and late patency of expanded polytetrafluoroethylene vascular grafts in aorta-coronary bypass. J Thorac Cardiovasc Surg 1981;81:860–864.
9. Anderson JM. Inflammatory response to implants. ASAIO Trans 1988;34:101–107.
10. Ratner B. Society for biomaterials 1992 presidential address: New ideas in biomaterials science—a path to engineered biomaterials. J Biomed Mater Res 1993;27:837–850.
11. Clowes AW, Kirkman TR, Reidy MA. Mechanisms of arterial graft healing: Rapid transmural capillary ingrowth provides a source of intimal endothelium and smooth muscle in porous PTFE prostheses. Am J Pathol 1986;123:220–230.
12. Sterpetti AV, Hunter WJ, Schultz RD, Farina C. Healing of high-porosity polytetrafluoroethylene arterial grafts is influenced by the nature of the surrounding tissue. Surgery 1992; 111:677–682.
13. Golden MA, Hanson SR, Kirkman TR, Schneider PA, Clowes AW. Healing of polytetrafluoroethylene arterial grafts is influenced by graft porosity. J Vasc Surg 1990;11:838–844.
14. Dellian M, Witwer BP, Salehi HA, Yuan F, Jain RK. Quantitation and physiological characterization of angiogenic vessels in mice: Effect of basic fibroblast growth factor, vascular endothelial growth factor/vascular permeability factor, and host microenvironment. Am J Pathol 1996;149:59–71.
15. Salzmann DL, Kleinert LB, Berman SS, Williams SK. Inflammation and neovascularization associated with clinically used vascular prosthetic materials. Cardiovasc Pathol 1999;8:63–71.
16. Williams SK, Berman SS, Kleinert LB. Differential healing and neovascularization of ePTFE implants in subcutaneous versus adipose tissue. J Biomed Mater Res 1997;35:473–481.
17. Rendell MS, Finnegan MF, Pisarri T, Healy JC, Lind A, Milliken BK, Finney DE, Bonner RF. A comparison of the cutaneous microvascular properties of the spontaneously hypertensive rat and the Wister-Kyoto rat. Comp Biochem Physiol 1999; 122:399–406.
18. Tedoriya T, Kawasuji M, Ueyama K, Sakakibara N, Takemura H, Watanabe E. Physiologic characteristics of coronary artery bypass grafts. Ann Thorac Surg 1993;56:951–956.
19. Hehrlein FW, Schlepper M, Loskot F, Scheld HH, Walter P, Mulch J. The use of expanded polytetrafluoroethylene (PTFE) grafts for myocardial revascularization. J Cardiovasc Surg 1984;25:549–553.
20. Hancock JB, Forshaw PL. Gore-Tex (polytetrafluoroethylene) in canine coronary artery bypass. J Thorac Cardiovasc Surg 1980;80:94–101.
21. Sunderkotter C, Goebeler M, Schulze-Osthoff K, Bhardwaj R, Sorg C. Macrophage-derived angiogenesis factors. Pharmacol Ther 1991;51:195–216.
22. Sunderkotter C, Steinbrink K, Goebeler M, Bhardwaj R, Sorg C. Macrophages and angiogenesis. J Leukoc Biol 1994;55:410–422.
23. Jackson JR, Seed MP, Kircher CH, Willoughby DA, Winkler JD. The codependence of angiogenesis and chronic inflammation. FASEB J 1997;11:457–465.
24. Folkman J. Angiogenesis in cancer, vascular, rheumatoid, and other disease. Nat Med 1995;1:27–31.